Eur J Nucl Med Mol Imaging (2011) 38:515–525
DOI 10.1007/s00259-010-1644-5

ORIGINAL ARTICLE

Decreased cerebral α4β2* nicotinic acetylcholine receptor availability in patients with mild cognitive impairment and Alzheimer's disease assessed with positron emission tomography

Kai Kendziorra · Henrike Wolf · Philipp Mael Meyer · Henryk Barthel · Swen Hesse · Georg Alexander Becker · Julia Luthardt · Andreas Schildan · Marianne Patt · Dietlind Sorger · Anita Seese · Herman-Josef Gertz · Osama Sabri

Received: 30 May 2010 / Accepted: 4 October 2010 / Published online: 11 November 2010

Abstract
Purpose Postmortem studies indicate a loss of nicotinic acetylcholine receptor (nAChRs) in Alzheimer's disease (AD). In order to establish whether these changes in the cholinergic system occur at an early stage of AD, we carried out positron emission tomography (PET) with a specific radioligand for the α4β2* nicotinic acetylcholine receptor (α4β2* nAChR) in patients with mild to moderate AD and in patients with amnestic mild cognitive impairment (MCI), who have a high risk to progress to AD.
Methods Nine patients with moderate AD, eight patients with MCI and seven age-matched healthy controls underwent 2-[^{18}F]fluoro-3-(2(*S*)-azetidinylmethoxy)pyridine (2-[^{18}F]FA-85380) PET. After coregistration with individual magnetic resonance imaging the binding potential (BP_{ND}) of 2-[^{18}F]FA-85380 was calculated using either the corpus callosum or the cerebellum as reference regions. PET data were analysed by region of interest analysis and by voxel-based analysis.
Results Both patients with AD and MCI showed a significant reduction in 2-[^{18}F]FA-85380 BP_{ND} in typical AD-affected brain regions. Thereby, the corpus callosum was identified as the most suitable reference region. The 2-[^{18}F]FA-85380 BP_{ND} correlated with the severity of cognitive impairment. Only MCI patients that converted to AD in the later course (n=5) had a reduction in 2-[^{18}F]FA-85380 BP_{ND}.
Conclusion 2-[^{18}F]FA-85380 PET appears to be a sensitive and feasible tool for the detection of a reduction in α4β2* nAChRs which seems to be an early event in AD. In addition, 2-[^{18}F]FA-85380 PET might give prognostic information about a conversion from MCI to AD.

Keywords Nicotinic acetylcholine receptors · 2-[^{18}F]FA-85380 · Alzheimer's disease · MCI · PET

The asterisk used in the receptor nomenclature means that the receptor complex may contain additional subunits.

K. Kendziorra (✉) · P. M. Meyer · H. Barthel · S. Hesse · G. A. Becker · J. Luthardt · A. Schildan · M. Patt · D. Sorger · A. Seese · O. Sabri
Department of Nuclear Medicine, University of Leipzig,
Liebigstr. 18,
04103 Leipzig, Germany
e-mail: K.Kendziorra@t-online.de

H. Wolf · H.-J. Gertz
Department of Psychiatry, University of Leipzig,
Semmelweisstr. 10,
04103 Leipzig, Germany

H. Wolf
Department of Old Age Psychiatry and Psychiatry Research,
Psychiatric University Hospital (PUK) Zurich,
University of Zurich,
Minervastr. 145,
8032 Zurich, Switzerland

Introduction

A dysfunction of acetylcholine transmitting neurons in the human brain is presumed to contribute substantially to the typical cognitive deficits observed in Alzheimer's disease (AD). The assumption of the cholinergic deficit in AD is based on various postmortem studies and has been referred to as the cholinergic hypothesis of AD [1]. This premise has since become an important working foundation for the majority of treatment strategies and drug development approaches for AD.

However, the initial studies providing the basis for the hypothesis were conducted using patients at relatively advanced stages of AD and could not gauge at which disease stage the cholinergic dysfunction occurred.

Recent postmortem and in vivo studies conducted in patients with mild cognitive impairment (MCI) or early-stage AD challenged the cholinergic hypothesis by revealing that cholinergic marker enzymes seem to be reduced only in advanced clinical stages [2] and may even be upregulated in earlier stages [3]. These findings were based on the activity of marker enzymes. To clarify the role of the cholinergic neurons in the course of AD, it is necessary to consider a wider range of abnormalities in the cholinergic system. Of the spectrum of known abnormalities in the cholinergic system in AD (alterations in neurotransmitter synthesis [4], receptor expression [5], neurotrophin support [6] and perhaps axonal transport [7]), decreases in nicotinic acetylcholine receptors (nAChR) are of particular interest. Neuronal nAChRs are transmitter-gated ion channels that are composed of different subunits [8]. Of the various subtypes, the α4β2* nAChR subtype is particularly important for brain imaging, since the α4β2* nAChR is the most abundant subtype in the human brain and the α4 subunit is most extensively reduced in several brain regions in AD [9].

The recent development of radiotracers based on 3-pyridyl ether compounds makes it possible to investigate the α4β2* nAChR in the living human brain. In this positron emission tomography (PET) study, we used the radiotracer 2-[^{18}F]fluoro-3-(2(*S*)-azetidinylmethoxy)pyridine (2-[^{18}F]FA-85380) [10]. In order to clarify whether nAChR changes occur early in the course of AD, we primarily examined AD patients with mild to moderate dementia and subjects with amnestic MCI, and compared them with normal age-matched healthy controls.

Materials and methods

Participants

The study population consisted of 17 non-smoking patients (9 patients with AD and 8 patients with MCI). None of the patients received anticholinergic or other centrally acting medication. None of the patients had a history of major psychiatric or neurological disorders other than dementia. As a control group seven age-matched, non-smoking healthy controls (HC) were examined.

The diagnosis of AD was made according to the NINCDS-ADRDA criteria. All AD patients had a typical clinical history with insidious onset of memory problems, parallelled by other cognitive deficits and impairment in activities of daily living. MCI was defined in accordance with recently published consensus criteria [11]. Objective cognitive impairment was defined as the performance of more than one standard deviation (SD) below age- and education-adjusted norms on neuropsychological tests and/or a Clinical Dementia Rating of 0.5. All subjects with MCI fulfilled the criteria for either "amnestic" (n=5) or "multidomain amnestic (n=3) MCI", according to the most recent consensus criteria [11]. Dementia was excluded based on the DSM-IV dementia criteria.

Cognitive deficits in memory and other cognitive domains were confirmed and quantified with the help of a standard neuropsychological test battery, comprising the Wechsler Logical Memory Scale and the Consortium to Establish a Registry for Alzheimer's Disease (CERAD) test battery. The Mini-Mental State Examination (MMSE) and the DemTect [12] were used as global measures of cognition. MCI patients were followed up over a mean period of 17 months (range 7–29 months).

Elderly control subjects were recruited through advertisement. Normal cognitive function was assured in the control subjects by MMSE performance >28 and DemTect global score within the normal range.

Written informed consent was obtained from all subjects; in patients with advanced cognitive decline additional written informed consent was obtained from caregivers, and the local Ethics Committee of the University of Leipzig, Germany approved the study protocol. All studies have therefore been performed in accordance with the ethical standards laid down in the 1964 Declaration of Helsinki.

Magnetic resonance imaging (MRI)

All participants underwent a structural T1-weighted MRI scan for anatomical coregistration with the individual PET image data and to rule out any pathologies except AD within 1 week from the PET scan. All MRI examinations were carried out on a 1.5-T MRI (MAGNETOM Symphony, Siemens, Erlangen, Germany). The image protocol consisted of a T1-weighted MPRANGE 3-D sequence [time of repetition 2,280 ms, time of echo 3.93.4 ms, 192 slices, field of view (FOV) 256 mm] and a T2-weighted turbo spin echo sequence (time of repetition 4,000 ms, time of echo 84 ms, 40 slices, slice thickness 3 mm, FOV 280 mm).

2-[^{18}F]FA-85380 PET

The 2-[^{18}F]FA-85380 was synthesized according to a protocol previously described in detail [13].

An ECAT EXACT HR+scanner [CTI/Siemens, Knoxville, TN, USA, 63 slices, resolution 4.7 mm full-width half-maximum (FWHM)], operating in 2-D acquisition mode, was

used for the PET data acquisition. 2-[^{18}F]FA-85380 was injected as a continuous short infusion over 90 s into the cubital vein. A tracer dose of 370 MBq was injected, which is equivalent to an amount of 2-[^{18}F]FA-85380 below 0.1 nmol/kg body weight. Serial PET scans were carried out over 120 min in 26 time frames (4×15 s, 4×1 min, 5×2 min, 5×5 min, 8×10 min). An additional 1-h scan (4×15 min) was started 6 h after tracer infusion. Attenuation correction factors were measured by means of a 20-min transmission scan acquired with three rotating ^{68}Ge sources before the start of the dynamic emission scans and the additional 1-h scan, respectively. An individual thermoplastic mask with a special head holder system was used to avoid head movement artefacts during the acquisition time and to guarantee exact repositioning of the individual's head in the late PET scan [14–16].

Blood sampling and analysis of individual binding of 2-[^{18}F]FA-85380

For input function measurement in all study subjects, arterial blood was obtained parallel to the PET scanning over a total time span of 7 h with 16 samples in the first 3 min post-tracer infusion (p.i.), followed by samples at 3, 4, 5, 6, 8, 10, 12, 14, 18, 25, 35, 50 and 60 min p.i. and thereafter every 30 min up to 7 h. The radioactivity in aliquots of plasma was measured using the Cobra gamma counter (Packard Instrument Company, Meriden, CT, USA).

The non-metabolized fraction of 2-[^{18}F]FA-85380 was measured for all subjects in the arterial blood samples, which were taken 14, 60, 120, 240, 330 and 420 min after radiotracer injection into the patients. Due to the slow metabolism of 2-[^{18}F]FA-85380 these time points were chosen. Plasma probes were deproteinized by perchloric acid and the intact 2-[^{18}F]FA-85380 was separated from its metabolites by HPLC, upon which separated sample fractions of 1.5 ml were collected and counted for radioactivity. The percentage of non-metabolized 2-[^{18}F]FA-85380 was calculated after data correction for the half-life time of ^{18}F and with respect to HPLC recovery.

The binding of 2-[^{18}F]FA-85380 to plasma proteins was determined for each patient individually using plasma samples (4×1 ml) obtained 3 min after administration of the radioligand, i.e. before the appearance of radiolabelled metabolites. For that purpose, plasma samples were applied to centrifugal filter devices (Centrifree®, Millipore, Bedford, MA, USA), equilibrated at 37°C and centrifuged for 6 min at 2,000 *g* to obtain the ultrafiltrate containing the free radioligand fraction. Before this approach was used, experimental analyses of plasma protein binding with human plasma that was added with 2-[^{18}F]FA-85380 were performed. For details see Sorger et al. [17, 18].

Estimation of PET parameters and image analysis

PMOD Version 2.5 (PMOD Technologies Ltd., Zurich, Switzerland) was used for kinetic data modelling. Due to the slow kinetics of 2-[^{18}F]FA-85380, PET studies should last up to 7 h for accurate quantification of 2-[^{18}F]FA-85380 binding by graphical analysis [19]. Parametric images of the regional 2-[^{18}F]FA-85380 distribution volume (2-[^{18}F]FA-85380 V_T) were calculated using the Logan plot (10 points between 1 h to 7 h p.i.) with the arterial input function corrected for decay, individual plasma protein binding and metabolites [19, 20]. Therefore, our V_T values differ from the values proposed by Innis et al. [21], where the input function used to compute the distribution volumes is not corrected for binding of tracer to plasma proteins. Our values of V_T are equal to V_T/f_p with f_p the free fraction of tracer in plasma [21]. The starting point of 1 h in the Logan plot analysis was used since linearity of the Logan plot was reached after 40–50 min in the thalamus as the region with highest α4β2* nAChR density.

Region of interest (ROI) analysis

The binding potential BP_{ND} [21] was calculated using the corpus callosum (CC) as a reference region, as previously published by our group in patients with Parkinson's disease [22]. Thereby, BP_{ND} is defined as the ratio of specifically bound radioligand to non-displaceable radioligand in tissue at equilibrium [21]. The CC has the lowest density of nAChRs in the human brain and the lowest 2-[^{18}F]FA-85380 V_T, and the tracer 2-[^{18}F]FA-85380 is almost non-displaceable by nicotine [23]. Therefore, as the most specific measure of the α4β2* nAChR availability, the binding potential BP_{ND} of the 2-[^{18}F]FA-85380 was calculated. For ROI analysis the 2-[^{18}F]FA-85380 V_T images were coregistered to an individual MRI using the mutual information algorithm implemented in the BRASS software (Hermes Medical Solutions, Stockholm, Sweden). Anatomical information from the individual MRI was used to manually trace irregular sets of single ROIs on two to three consecutive transverse slices. ROIs were carefully drawn only in areas containing brain tissue in the MRI scan, thereby minimizing partial volume effects. These MRI-defined ROIs were overlaid onto the PET data set. A priori hypothesis-driven ROIs were selected according to the results of prior postmortem studies demonstrating nAChR reductions in AD and MCI in the frontal, parietal and temporal cortex, the striatum and in the hippocampus. In addition, thalamus, anterior and posterior cingulate cortices were chosen, because they are known to be affected in AD. Furthermore, in order to assess 2-[^{18}F]FA-85380 BP_{ND} in regions that are not typically affected by AD pathology, the occipital cortex and cerebellum were analysed as control regions.

Statistical analysis

For statistical comparison of the groups, the Mann-Whitney U test was used since the assumptions of the test, i.e. random samples, independence within the samples and mutual independence between samples, were fulfilled.

For group comparisons a reduction of 2-[^{18}F]FA-85380 BP_{ND} in a priori defined ROIs was assumed in frontal, parietal and temporal cortex, the striatum, the hippocampus, the thalamus, and the anterior and posterior cingulate cortices, in accordance with postmortem data in AD as mentioned above. Therefore, a correction for multiple comparison was voided and a significance level at $p<0.05_{uncorrected}$ was accepted.

Correlations between cognitive scores (MMSE, DemTect) and 2-[^{18}F]FA-85380 BP_{ND} assessed by ROI analysis in the regions typically affected by AD pathology were calculated in the whole study group by means of Spearman rank correlation analysis. The significance level was accepted at $p<0.05$.

Statistical analysis was undertaken with the help of the SPSS software package, version 14.0 (SPSS, Chicago, IL, USA).

Voxel-based analysis

For exploratory analysis of differences between HC and AD/MCI patients a voxel-wise statistical analysis of the 2-[^{18}F]FA-85380 V_T images was performed using SPM99 (Statistical Parametric Mapping software, Wellcome Department of Cognitive Neurology, London, UK), implemented in MATLAB 6.5.0 (The MathWorks, Inc., Natick, MA, USA). No proportional scaling was applied.

In addition, 2-[^{18}F]FA-85380 distribution volume ratios ($DVR=BP_{ND}+1$) were calculated and analysed by SPM99 in accordance with Terrière et al. [24]. 2-[^{18}F]FA-85380 DVR were calculated by scaling 2-[^{18}F]FA-85380 V_T to the CC or the cerebellum, respectively. To calculate DVR, values for the CC and the cerebellum were obtained by ROI analysis (Hermes Medical Solutions, Stockholm, Sweden). For SPM99 analysis all brain images of AD, MCI and HC were spatially normalized to the Talairach space on the [^{15}O]H_2O SPM PET template and smoothed with a 12-mm FWHM Gaussian kernel in order to adjust the anatomical variability between the individual brains and to enhance the signal to noise ratio for the analysis.

For exploratory SPM analysis, carried out for group comparisons, a relatively high significance level without controlling for multiple comparisons was accepted. SPM analysis was performed using a two-sample t test and considered significant for $p<0.005$ (uncorrected; minimum cluster size 30 voxels; voxel size 2×2×2 mm). The brain areas with decreased or increased 2-[^{18}F]FA-85380 DVR were detected by using different contrast vectors (HC>AD: 1 −1 0; HC<AD: −1 1 0/HC>MCI: 1 −1 0; HC<MCI: −1 1 0) and imaged on a glass brain, three-dimensional brain images or transaxial brain slices. Furthermore, the significantly different brain areas were displayed with Montreal Neurological Institute (MNI) coordinates in the stereotactic space of Talairach using the automated anatomical labelling (local maxima labelling) function of SPM99 [25].

Results

Subjects

Table 1 shows the demographic characteristics of the subjects. Groups were similar with respect to age and

Table 1 Demographic and clinical characteristics of subjects studied with 2-[^{18}F]FA-85380 PET

	Controls	MCI	AD	Significance
n	7	8	9	
Sex (M:F)	3:4	5:3	5:4	NS
Age	60.7 (9.0)	60.7 (6.5)	65.5 (6.5)	NS
MMSE (max. 30)	29.6 (0.8)	26.8 (1.7)	18.3 (5.8)	0.002[a]; <0.001[b]
DemTect (max. 18)	16.4 (2.1)	12.1 (2.7)	5.6 (3.2)	0.009[a]; <0.001[b]
Clock drawing test	1	2.7 (1.5)	4.0 (1.4)	<0.04[a]; <0.001[b]
Duration (month)		47.7 (42.5)	35.5 (15.3)	
AChEI	0	0	0	
Other centrally acting medication	0	0	0	
Nicotine abuse	0	0	0	

Values expressed as mean (SD). Significance testing was done by pairwise Mann-Whitney U test

AD Alzheimer's disease, *MCI* mild cognitive impairment, *MMSE* Mini-Mental State Examination, *NS* not significant, *AChEI* acetylcholinesterase inhibitors

[a] Significant difference between normal controls and MCI

[b] Significant difference between normal controls and AD

gender, although the AD patients tended to be older. As expected MMSE and DemTect scores in patients with AD or MCI were lower than in controls, and the clock drawing test was normal in all HC (value of 1) with pathological values in the AD group, respectively. Clinical follow-up over a mean period of 17 months (range 7–29 months) revealed a conversion to AD in five of the eight MCI patients (three amnestic MCI and two multidomain amnestic MCI). These were classified as converters (MCI-C), whereas three MCI patients showed stable disease (MCI-S).

2-[^{18}F]FA-85380 plasma protein binding and metabolites

There was no significant difference according to plasma protein binding of 2-[^{18}F]FA-85380 in arterial plasma between the groups. Plasma protein binding of 2-[^{18}F]FA-85380 was low at 17±4% and did not show significant differences between the groups. On average the non-metabolized 2-[^{18}F]FA-85380 in plasma tended to be lower in patients than in HC at later time points (>120 min p.i.); however, a high interindividual variability of the data was observed. For details see Sorger et al. [17, 18].

2-[^{18}F]FA-85380 BP_{ND} in the brains of normal controls

In our normal control subjects, the 2-[^{18}F]FA-85380 BP_{ND} in the human brain was highest in the thalamus (mean±SD 1.8±0.4), intermediate in cortical regions (0.4±0.1), in the striatum [caudate nucleus (0.7±0.2), putamen (0.7±0.2)] and in the cerebellum (0.6±0.3) (Table 2).

2-[^{18}F]FA-85380 V_T in the CC showed no significant difference between the three groups (HC 4.0±0.6, MCI patients 4.5±0.3, AD patients 4.6±0.3; p=0.72 AD vs HC and p=0.53 MCI vs HC).

Group differences in 2-[^{18}F]FA-85380 BP_{ND}: ROI analysis

Table 2 shows the mean of 2-[^{18}F]FA-85380 BP_{ND} within each ROI for controls, patients with AD and patients with MCI. There was a significantly reduced 2-[^{18}F]FA-85380 BP_{ND} in AD compared to HC in the frontal and temporal cortex bilaterally, the posterior cingulate cortex bilaterally, the right hippocampus, the left caudate head and the right anterior cingulate cortex. In MCI patients significantly reduced 2-[^{18}F]FA-85380 BP_{ND} was found in the frontal cortex bilaterally, the right parietal cortex, the left temporal

Table 2 BP_{ND} of 2-[^{18}F]FA-85380 in different brain regions for healthy controls, patients with Alzheimer's dementia (AD) and patients with MCI

	Controls (n=7)	MCI (n=8)	AD (n=9)	Significance
R frontal	0.37 (0.11)	0.20 (0.07)	0.21 (0.09)	<0.01[a], <0.005[b]
L frontal	0.34 (0.13)	0.18 (0.08)	0.19 (0.11)	<0.01[a], <0.005[b]
R parietal	0.35 (0.14)	0.21 (0.09)	0.25 (0.13)	<0.05[a]
L parietal	0.36 (0.12)	0.23 (0.10)	0.25 (0.09)	
R temporal	0.32 (0.16)	0.19 (0.11)	0.14 (0.08)	<0.005[b]
L temporal	0.34 (0.11)	0.17 (0.08)	0.16 (0.10)	<0.01[a], <0.001[b]
R occipital	0.32 (0.14)	0.18 (0.10)	0.21 (0.11)	
L occipital	0.32 (0.16)	0.22 (0.11)	0.23 (0.13)	
R cerebellum	0.58 (0.27)	0.45 (0.06)	0.45 (0.13)	
L cerebellum	0.56 (0.31)	0.42 (0.11)	0.46 (0.14)	
R hippocampus	0.50 (0.16)	0.23 (0.14)	0.27 (0.18)	<0.01[a], <0.005[b]
L hippocampus	0.45 (0.19)	0.30 (0.09)	0.26 (0.17)	
R anterior cingulate	0.40 (0.18)	0.29 (0.05)	0.19 (0.12)	<0.005[b]
L anterior cingulate	0.41 (0.12)	0.32 (0.13)	0.28 (0.11)	
R post. cingulate	0.55 (0.14)	0.39 (0.14)	0.27 (0.13)	<0.05[a], <0.001[b]
L post. cingulate	0.55 (0.14)	0.38 (0.16)	0.31 (0.15)	<0.001[b]
R caudate	0.77 (0.21)	0.38 (0.23)	0.36 (0.18)	<0.05[a], <0.001[b]
L caudate	0.58 (0.15)	0.29 (0.20)	0.33 (0.22)	<0.05[a]
R putamen	0.70 (0.24)	0.63 (0.16)	0.62 (0.20)	
L putamen	0.69 (0.21)	0.63 (0.14)	0.64 (0.24)	
R thalamus	1.79 (0.39)	1.86 (0.54)	1.56 (0.57)	
L thalamus	1.88 (0.50)	1.83 (0.58)	1.53 (0.52)	
Brainstem	0.88 (0.33)	0.67 (0.16)	0.66 (0.23)	
R periventricular white matter	0.66 (0.22)	0.67 (0.13)	0.64 (0.22)	
L periventricular white matter	0.67 (0.18)	0.69 (0.20)	0.64 (0.22)	

Significance testing was done by pairwise Mann-Whitney U test. Values expressed as mean (SD)

[a] Significant difference between normal controls and MCI

[b] Significant difference between normal controls and AD

cortex, the right hippocampus, caudate head bilaterally and the right posterior cingulate cortex. A subgroup analysis of MCI-C and MCI-S patients revealed a significantly reduced 2-[^{18}F]FA-85380 BP_{ND} in the aforementioned and additional brain areas, whereas MCI-S patients showed no brain areas with a significantly reduced 2-[^{18}F]FA-85380 BP_{ND} (Table 3).

Group differences in 2-[^{18}F]FA-85380 DVR: SPM analysis

An explorative SPM analysis was performed to detect further regions with reduced 2-[^{18}F]FA-85380 binding.

There were no significant differences for the analysis of 2-[^{18}F]FA-85380 V_T images between HC and AD or MCI patients.

Analysing 2-[^{18}F]FA-85380 DVR by using the CC as a reference region (2-[^{18}F]FA-85380 DVRcc) exploratory SPM99 analysis revealed significantly lower 2-[^{18}F]FA-85380 DVR in AD compared to HC in the precuneus/posterior cingulate cortex, the left thalamus, right hippocampus/parahippocampal, the temporal cortex and frontal cortex bilaterally, and the left caudate head at $p<0.005_{uncorrected}$. In MCI patients significantly reduced 2-[^{18}F]FA-85380 DVRcc was found in the precuneus/posterior cingulate cortex, right hippocampus/parahippocampal, the frontal cortex, the superior temporal gyrus bilaterally and the superior frontal gyrus bilaterally at $p<0.005_{uncorrected}$ (Fig. 1, left column). These findings could be reproduced in smaller clusters with $p<0.001_{uncorrected}$ (Fig. 1, right column).

Using the cerebellum as a reference region, exploratory SPM99 analysis of 2-[^{18}F]FA-85380 DVRce at $p<0.005_{uncorrected}$ demonstrated significantly lower 2-[^{18}F]FA-85380 DRVce in AD and MCI patients in similar regions (AD: right precuneus/posterior cingulate cortex and thalamus bilaterally; MCI: precuneus/posterior cingulate cortex and temporal cortex, respectively), however, compared to the results of the SPM analysis of 2-[^{18}F]FA-85380 DVRcc between HC and AD or MCI at $p<0.005_{uncorrected}$ to a smaller extent. The extent of significantly reduced 2-[^{18}F]FA-85380 DVRce in AD and MCI at $p<0.005_{uncorrected}$ was approximately similar to the extent of significantly lower 2-[^{18}F]FA-85380 DVRcc in AD and MCI at $p<0.001_{uncorrected}$ (Fig. 1, middle and right columns).

A SPM99 subgroup analysis of the 2-[^{18}F]FA-85380 DVRcc of MCI-C patients and the MCI-S patients compared to the healthy controls revealed at most very small clusters of lower 2-[^{18}F]FA-85380 DVRcc between

Table 3 BP_{ND} of 2-[^{18}F]FA-85380 in different brain regions for healthy controls, patients with MCI converting to AD (MCI-C) and MCI-patients with stable cognitive course (MCI-S)

	Controls (n=7)	MCI-C (n=5)	MCI-S (n=3)
R frontal	0.37 (0.11)	0.15 (0.03)**	0.27 (0.06)
L frontal	0.34 (0.13)	0.15 (0.06)*	0.23 (0.09)
R parietal	0.35 (0.14)	0.17 (0.05)*	0.27 (0.10)
L parietal	0.36 (0.12)	0.18 (0.08)*	0.31 (0.09)
R temporal	0.32 (0.16)	0.11 (0.05)*	0.31 (0.05)
L temporal	0.34 (0.11)	0.12 (0.06)**	0.25 (0.03)
R occipital	0.32 (0.14)	0.13 (0.07)*	0.27 (0.08)
L occipital	0.32 (0.16)	0.16 (0.04)*	0.31 (0.13)
R cerebellum	0.58 (0.27)	0.40 (0.03)	0.52 (0.03)
L cerebellum	0.56 (0.31)	0.35 (0.06)	0.53 (0.07)
R hippocampus	0.50 (0.16)	0.18 (0.07)**	0.30 (0.20)
L hippocampus	0.45 (0.19)	0.30 (0.11)	0.28 (0.17)
R anterior cingulate	0.40 (0.18)	0.29 (0.04)	0.29 (0.08)
L anterior cingulate	0.41 (0.12)	0.24 (0.05)*	0.46 (0.07)
R post. cingulate	0.55 (0.14)	0.29 (0.04)**	0.55 (0.06)
L post. cingulate	0.55 (0.14)	0.29 (0.04)**	0.53 (0.18)
R caudate	0.77 (0.21)	0.26 (0.11)**	0.58 (0.27)
L caudate	0.58 (0.15)	0.20 (0.09)**	0.43 (0.26)
R putamen	0.70 (0.24)	0.53 (0.06)	0.79 (0.13)
L putamen	0.69 (0.21)	0.58 (0.08)	0.71 (0.20)
R thalamus	1.79 (0.39)	1.57 (0.43)	2.32 (0.33)
L thalamus	1.88 (0.50)	1.51 (0.41)	2.36 (0.42)
Brainstem	0.88 (0.33)	0.56 (0.05)	0.85 (0.06)
R periventricular white matter	0.66 (0.22)	0.61 (0.11)	0.77 (0.10)
L periventricular white matter	0.67 (0.18)	0.62 (0.19)	0.80 (0.19)

Significance testing was done by pairwise Mann-Whitney U test. Significant difference between normal controls and MCI-C, *p <0.05; **p<0.005. No significant difference between normal controls and MCI-S was observed. Values expressed as mean (SD)

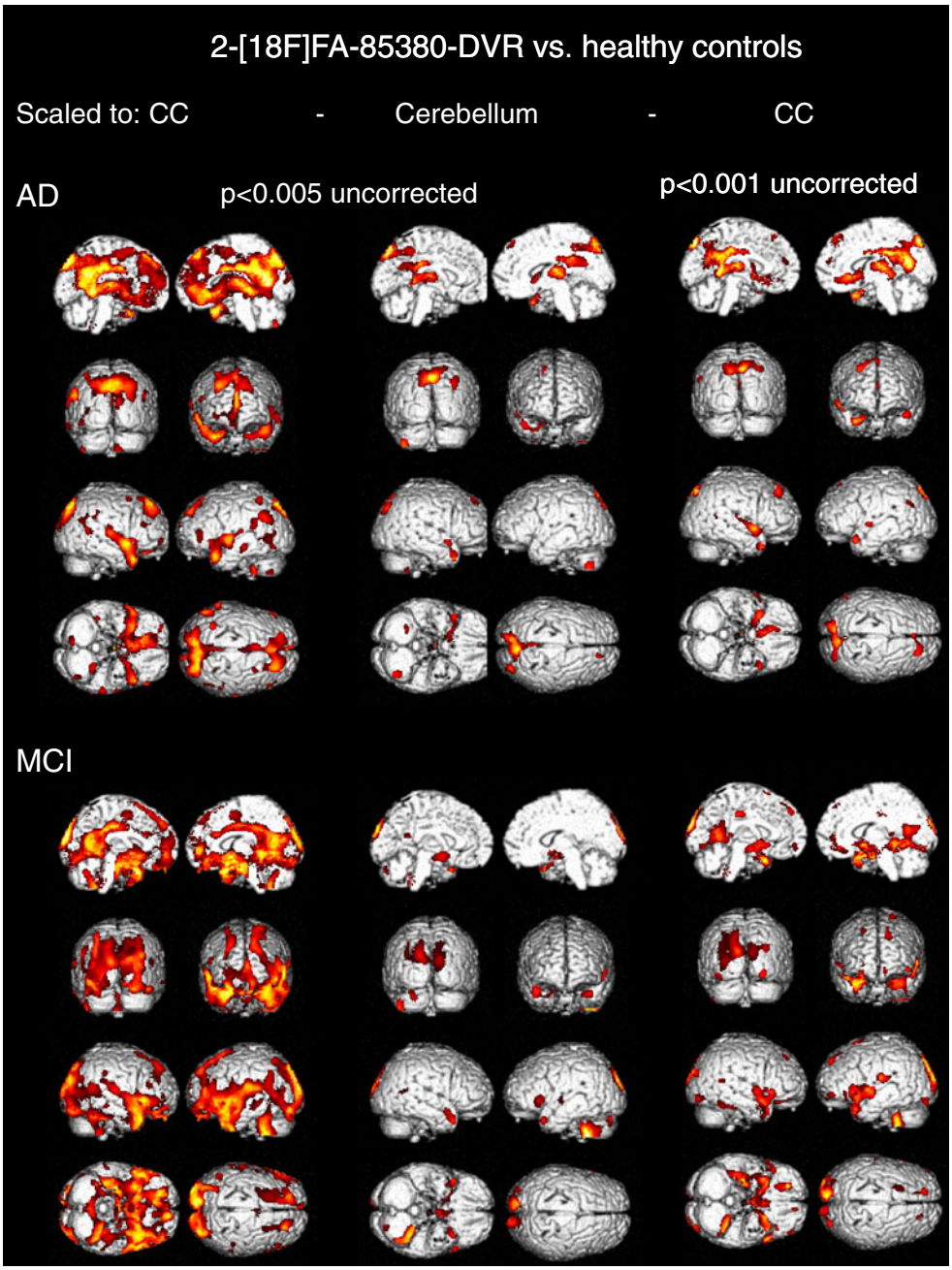

Fig. 1 SPM projections onto standard template of clusters, where the 2-[^{18}F]FA-85380 distribution volume ratio is significantly decreased in AD patients and MCI patients compared with healthy control subjects. Data were scaled to the corpus callosum (CC) and the cerebellum as reference region. Medial views (*top*), posterior view (*second row left*), anterior view (*second row right*), lateral views (*third row*), inferior view (*bottom left*) **and superior view (***bottom right***)**

healthy controls and MCI-S patients, whereas MCI-C patients showed significantly ($p<0.005_{\text{uncorrected}}$) reduced 2-[^{18}F]FA-85380 DVRcc in regions similar to those found for the comparison between healthy controls and AD at $p<0.005_{\text{uncorrected}}$ (Fig. 2 and Fig. 1, left column).

Relationship between regional 2-[^{18}F]FA-85380 BP_{ND} (ROI analysis) and severity of cognitive symptoms

Spearman correlation analyses yielded significant ($p<0.05_{\text{uncorrected for multiple comparisons}}$) correlations between the cognitive performance as scored by means of the MMSE and the 2-[^{18}F]FA-85380 BP_{ND} in the following brain regions: right caudate, temporal and posterior cingulate cortex bilaterally, and right anterior cingulate cortex. Correlation coefficients ranged from 0.39 (right anterior cingulate cortex) to 0.56 (left posterior cingulate cortex). Furthermore, significant positive correlations between the DemTect score and the 2-[^{18}F]FA-85380 BP_{ND} were observed in the caudate head bilaterally, the frontal, temporal and posterior cingulate cortex bilaterally, and the left anterior cingulate cortex, ranging from 0.38 (left anterior cingulate cortex) to 0.61 (left posterior cingulate cortex). Figure 3 shows the relationship between the DemTect score and the 2-[^{18}F]FA-85380 BP_{ND} in the caudate head and the frontal, temporal and posterior

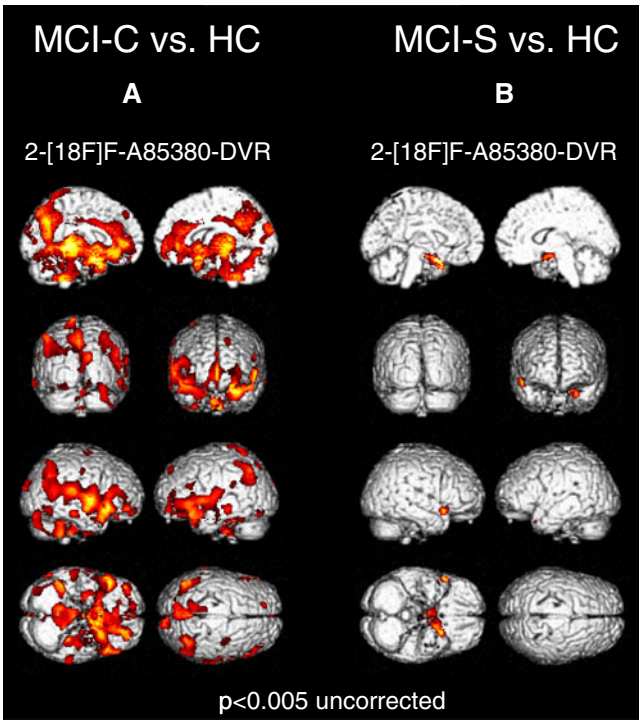

Fig. 2 SPM projections onto standard template of clusters, where the 2-[^{18}F]FA-85380 distribution volume ratio is significantly decreased in the MCI patients who converted to AD (MCI-C) patients compared with healthy control subjects (**a**), while stable MCI patients (MCI-S) show only minor changes (**b**). Medial views (*top*), posterior view (*second row left*), anterior view (*second row right*), lateral views (*third row*), inferior view (*bottom left*) and superior view (*bottom right*)

cingulate cortex in our study cohort. However, in this small sample size there were no significant correlations between the 2-[^{18}F]FA-85380 BP_{ND} and cognitive sub-functions like memory or recall assessed by sub-scores in the DemTect or to the CERAD test battery or the Wechsler Logical Memory Scale in any of the brain regions.

Discussion

This study provides in vivo support for an early reduction of α4β2* nAChRs in the onset of AD by revealing a significant reduction of 2-[^{18}F]FA-85380 binding in patients with MCI and in early dementia in AD. Our study included eight patients with amnestic MCI, patients who have a high likelihood to progress to AD, as was the case in five of the MCI patients. The lack of further cognitive decline in the three MCI patients with normal α4β2* nAChR availability in our study supports the aetiological heterogeneity of MCI. Since postmortem analysis of the cholinergic neurons suggests the existence of a critical neuron loss as a threshold between normal aging and AD [26], this finding could be a hint that 2-[^{18}F]FA-85380 PET might give prognostic information about a conversion from MCI to AD. Our findings suggest that the reduced α4β2* nAChR binding may be a very early marker in the course of AD. These data are supported by recent autoradiographic investigations showing that α4β2* nAChR deficits in AD brains represent an early phenomenon in the course of the disease [26]. The topographical pattern of the α4β2* nAChR reduction detected in the AD and MCI patients in our study is supported by postmortem studies in AD. These studies revealed significant α4β2* nAChR deficits (up to 75% as compared to normal controls) in the temporal and frontal cortex, in the hippocampus and in the caudate nucleus of AD patients [27–30]. In our study, significantly reduced α4β2* nAChRs within the a priori selected ROIs were expected and proven in the frontal cortex bilaterally, the temporal cortex bilaterally, the posterior cingulate cortex bilaterally, the caudate nucleus bilaterally, and the right hippocampus and anterior cingulate cortex in AD patients. Similar reductions were seen in MCI patients. The results from the a priori ROI analysis could be reproduced by explorative voxel-based analysis using SPM99.

Our results are in line with studies using the PET tracer [^{11}C]nicotine, and more recently, the single photon emission computed tomography (SPECT) tracer [^{123}I]-5-iodo-3-[2(*S*)-2-azetidinylmethoxy]pyridine ([^{123}I]-5IA-85380) for in vivo imaging of α4β2* nAChRs in patients with AD and MCI [24, 31, 32]. In [^{11}C]nicotine PET studies a significantly lower [^{11}C]nicotine binding was observed in the brain of AD patients with mild to moderate dementia compared to healthy controls [31, 33], especially in the frontal cortex, temporal cortex and hippocampus [31]. Studies using the SPECT tracer [^{123}I]-5IA-85380 and scaling to a reference region could also demonstrate a significant reduction of tracer uptake in the frontal cortex, the right medial temporal cortex, the striatum and the pons in AD and in the medial temporal cortex in MCI [24, 32].

In contrast, one recently published PET study using 2-[^{18}F]FA-85380 [34] and one SPECT study using [^{123}I]-5IA-85380 [35] in early AD patients could not detect significant differences in the α4β2* nAChR availability between patients and healthy controls. In addition to different study populations, the divergent results among the published in vivo studies might be related to different quantification methods. While differences in nAChR availability between healthy controls and patients could be observed in the SPECT studies that performed scaling to a reference region [24, 32], the study by Mitsis et al. [35] could not reproduce the results by using a bolus-infusion protocol. In the PET study a simplified modelling method without arterial blood samples was used and normalization to a reference region was not performed. In line with these studies, we could detect no significant differences between HC and AD or MCI patients, respectively, when analysing 2-[^{18}F]FA-85380 V_T with SPM99 or ROI analysis, possibly due to (1) the small sample size, (2) a

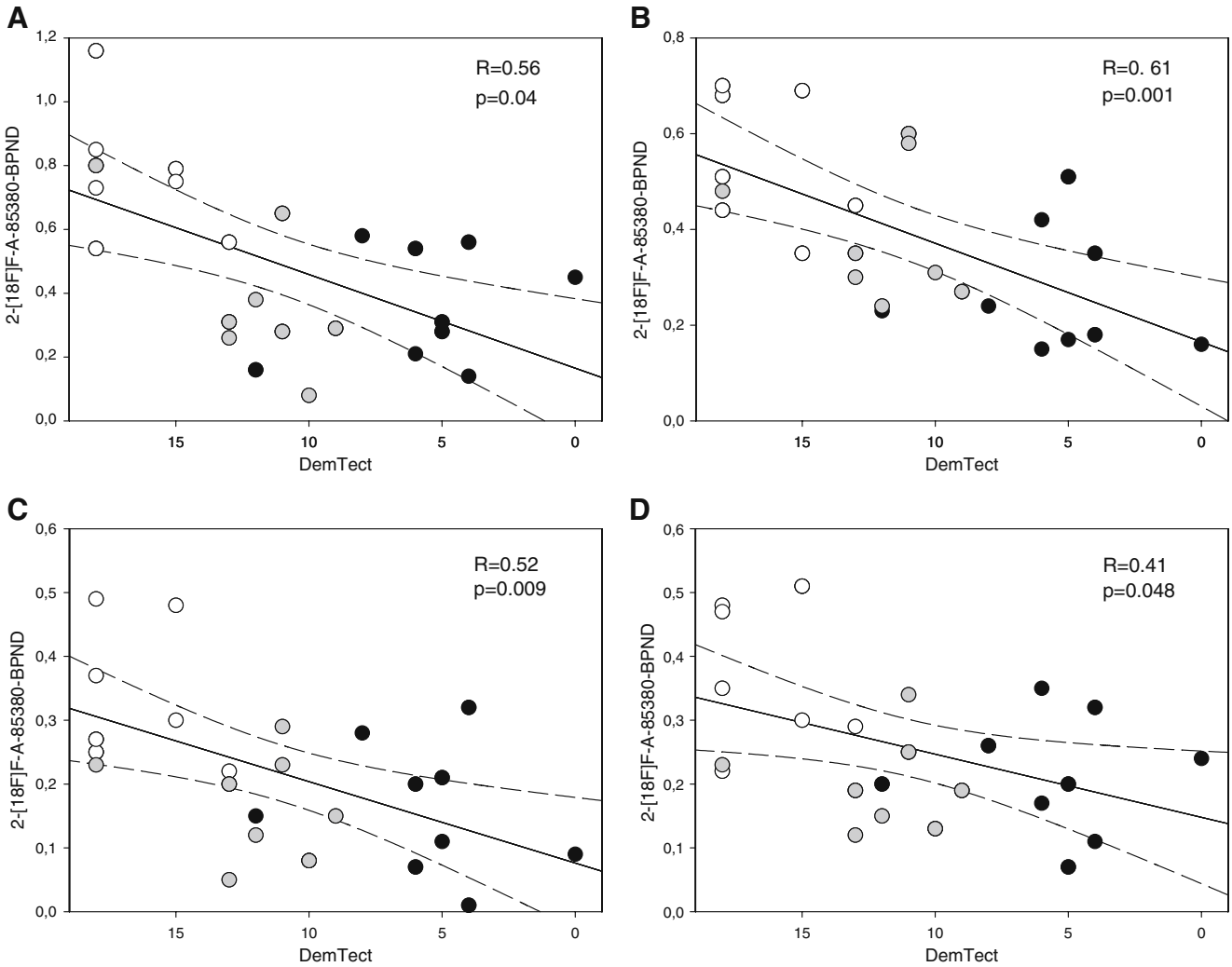

Fig. 3 Correlation between 2-[^{18}F]FA-85380 BP_{ND} and DemTect in the four brain areas with the highest correlations **a** Right caudate head. **b** Right posterior cingulate cortex. **c** Left temporal cortex. **d** Right frontal cortex. *Open circle* healthy controls, *grey circle* MCI, *black circle* AD

relatively high interindividual variability of 2-[^{18}F]FA-85380 V_T and (3) a relatively high amount of nonspecific binding of 2-[^{18}F]FA-85380 that masks group differences in small sample sizes. However, it is well known that the group variability can be reduced using an appropriate reference region [36]. The normalization of regional 2-[^{18}F]FA-85380 V_T to a reference region (cerebellum or CC), as performed in this study and thus gaining DVR values, therefore serves to minimize the influence of interindividual variability and allows better detection of potential group differences.

Using DVR values in brain studies exactly eliminates a constant multiplicative error in the input function. It can therefore be expected that DVR are less affected by measurements of the amount of unmetabolized parent compound. Since f_p is a multiplicative factor in the input function, DVR gets independent of the individual f_p value and noise associated with its measurement.

Choosing the right reference region is of extreme importance when calculating DVR. Although white matter reference regions have been used in quantification of neuroreceptors before [37], one cannot rule out differences in unspecific binding between the reference region and the grey matter cortical brain areas in individual subjects or between the groups analysed. However, we could detect differences in similar regions between the groups by using the CC and the cerebellum as reference regions with a higher magnitude by using the CC. Since the CC has the lowest density of α4β2* nAChRs in the human brain and the lowest 2-[^{18}F]FA-85380 V_T, and since the 2-[^{18}F]FA-85380 binding in the CC is almost non-displaceable by nicotine [23], the effect of small differences of 2-[^{18}F]FA-85380 V_T in the CC between the groups is less likely to have an impact on results found compared to other, receptor-rich areas like the cerebellum or whole grey matter normalization. We therefore assume that our findings are due to a true reduction

in α4β2* nAChR in the grey matter in AD and MCI patients and not due to differences in unspecific binding between the three groups.

While using the CC as a reference region would greatly simplify quantification of [^{123}I]-5IA-85380 uptake [38], its drawbacks like relatively small size and direct neighbourhood to the ventricle makes it difficult to use during quantification in SPECT studies. Previous SPECT studies showing α4β2* nAChR reductions in AD and MCI patients have therefore used the cerebellum as a reference region [24, 32, 33, 39]. We could also detect significant group differences using the cerebellum as a reference region, which were observed in the same brain regions as in the CC scaled analysis. However, the magnitude of group differences in our study was higher using CC scaled data. This could be due to the fact that the human cerebellum contains α4β2* nAChRs [23, 40]. Given the higher spatial resolution of PET compared to SPECT and using individual coregistered MRIs to define the outline and thus minimizing spillover effects, using the CC as a reference region in PET studies seems to be more suitable to detect reduced α4β2* nAChR availability in AD/MCI compared to HC.

There was a weak correlation between the global cognitive performance, assessed by MMSE and DemTect, and the α4β2* nAChR availability in brain regions known to be affected in AD if the whole study group was analysed. Hereby, both the MMSE and the DemTect showed similar correlation coefficients. This finding could indicate a stage sensitivity of the α4β2* nAChR decline as previously reported with [^{11}C]nicotine [31]. However, the correlation was not significant in the AD or MCI group alone, possibly due to the small sample size, and the restricted variability in neuropsychological performance. We could not observe a significant correlation between the α4β2* nAChR availability in brain regions and cognitive sub-functions assessed by sub-scores in the DemTect like memory or recall, the CERAD test battery or the Wechsler Logical Memory Scale, respectively, maybe due to the small number of patients in the study.

Atrophy in AD and consecutive atrophy effects on the PET data are important factors that need to be considered in interpreting these measurements. However, we intentionally did not make use of an automated atrophy correction method in order to avoid the fundamental problem of overcorrection in this case. To minimize atrophy effects, we defined irregular, exclusively relevant brain tissue-containing ROIs based on the individual MRI after PET vs MRI coregistration. Since a reduction in α4β2* nAChRs can also be verified in MCI patients, who had no cerebral atrophy in our cases, we are confident that the results obtained in the AD patient group are primarily not an atrophy effect. However, we cannot rule out an involvement of atrophy effects on the results of the AD group entirely.

In conclusion, this study gives in vivo indication of an early affection of α4β2* nAChRs in AD. Decrease in α4β2* nAChR binding can be detected already in MCI. 2-[^{18}F]FA-85380 PET appears to be a sensitive and feasible tool for the detection of pathophysiologically relevant receptor changes in the cholinergic system. In addition, 2-[^{18}F]FA-85380 PET might give prognostic information about a conversion from MCI to AD.

Funding This study was funded by the University of Leipzig; there was no involvement in the study design; in the collection, analysis and interpretation of the data; in the writing of the report; and in the decision to submit the paper for publication.

Conflict of interest None.

References

1. Bartus RT, Dean RL, Beer B, Lippa AS. The cholinergic hypothesis of geriatric memory dysfunction. Science 1982;217:408–17.
2. Davis KL, Mohs RC, Marin D, Purohit DP, Perl DP, Lantz M, et al. Cholinergic markers in elderly patients with early signs of Alzheimer disease. JAMA 1999;281:1401–6.
3. DeKosky ST, Ikonomovic MD, Styren SD, Beckett L, Wisniewski S, Bennett DA, et al. Upregulation of choline acetyltransferase activity in hippocampus and frontal cortex of elderly subjects with mild cognitive impairment. Ann Neurol 2002;51:145–55.
4. Bowen DM, Benton JS, Spillane JA, Smith CC, Allen SJ. Choline acetyltransferase activity and histopathology of frontal neocortex from biopsies of demented patients. J Neurol Sci 1982;57:191–202.
5. Whitehouse PJ, Martino AM, Antuono PG, Lowenstein PR, Coyle JT, Price DL, et al. Nicotinic acetylcholine binding sites in Alzheimer's disease. Brain Res 1986;371:146–51.
6. Phillips HS, Hains JM, Armanini M, Laramee GR, Johnson SA, Winslow JW. BDNF mRNA is decreased in the hippocampus of individuals with Alzheimer's disease. Neuron 1991;7:695–702.
7. Dai J, Buijs RM, Kamphorst W, Swaab DR. Impaired axonal transport of cortical neurons in Alzheimer's disease is associated with neuropathological changes. Brain Res 2002;948:138–44.
8. Lindstrom J, Anand R, Peng X, Gerzanich V, Wang F, Li Y. Neuronal nicotinic receptor subtypes. Ann N Y Acad Sci 1995;757:100–16.
9. Martin-Ruiz CM, Court JA, Molnar E, Lee M, Gotti C, Mamalaki A, et al. Alpha4 but not alpha3 and alpha7 nicotinic acetylcholine receptor subunits are lost from the temporal cortex in Alzheimer's disease. J Neurochem 1999;73:1635–40.
10. Horti AG, Scheffel U, Koren AO, Ravert HT, Mathews WB, Musachio JL, et al. 2-[18F]Fluoro-A-85380, an in vivo tracer for the nicotinic acetylcholine receptors. Nucl Med Biol 1998;25:599–603.
11. Winblad B, Palmer K, Kivipelto M, Jelic V, Fratiglioni L, Wahlund LO, et al. Mild cognitive impairment—beyond controversies, towards a consensus: report of the International Working Group on Mild Cognitive Impairment. J Intern Med 2004;256:240–6.
12. Kessler J, Calabrese P, Kalbe E, Berger F. DemTect: a new dementia screening instrument. Psycho 2000;26:343–7.

13. Schildan A, Patt M, Sabri O. Synthesis procedure for routine production of 2-[18F]fluoro-3-(2(S)-azetidinylmethoxy)pyridine (2-[18F]F-A-85380). Appl Radiat Isot 2007;65:1244–8.
14. Sabri O, Erkwoh R, Schreckenberger M, Owega A, Sass H, Buell U. Correlation of positive symptoms exclusively to hyperperfusion or hypoperfusion of cerebral cortex in never-treated schizophrenics. Lancet 1997;349:1735–9.
15. Sabri O, Ringelstein EB, Hellwig D, Schneider R, Schreckenberger M, Kaiser HJ, et al. Neuropsychological impairment correlates with hypoperfusion and hypometabolism but not with severity of white matter lesions on MRI in patients with cerebral microangiopathy. Stroke 1999;30:556–66.
16. Sabri O, Owega A, Schreckenberger M, Sturz L, Fimm B, Kunert P, et al. A truly simultaneous combination of functional transcranial Doppler sonography and H(2)(15)O PET adds fundamental new information on differences in cognitive activation between schizophrenics and healthy control subjects. J Nucl Med 2003;44:671–81.
17. Sorger D, Becker GA, Hauber K, Schildan A, Patt M, Birkenmeier G, et al. Binding properties of the cerebral alpha4beta2 nicotinic acetylcholine receptor ligand 2-[18F]fluoro-A-85380 to plasma proteins. Nucl Med Biol 2006;33:899–906.
18. Sorger D, Becker GA, Patt M, Schildan A, Grossmann U, Schliebs R, et al. Measurement of the alpha4beta2* nicotinic acetylcholine receptor ligand 2-[(18)F]fluoro-A-85380 and its metabolites in human blood during PET investigation: a methodological study. Nucl Med Biol 2007;34:331–42.
19. Chefer SI, London ED, Koren AO, Pavlova OA, Kurian V, Kimes AS, et al. Graphical analysis of 2-[18F]FA binding to nicotinic acetylcholine receptors in rhesus monkey brain. Synapse 2003;48:25–34.
20. Gallezot JD, Bottlaender MA, Delforge J, Valette H, Saba W, Dollé F, et al. Quantification of cerebral nicotinic acetylcholine receptors by PET using 2-[18F]fluoro-A-85380 and the multi-injection approach. J Cereb Blood Flow Metab 2008;28:172–89.
21. Innis RB, Cunningham VJ, Delforge J, Fujita M, Gjedde A, Gunn RN, et al. Consensus nomenclature for in vivo imaging of reversibly binding radioligands. J Cereb Blood Flow Metab 2007;27:1533–39.
22. Meyer PM, Strecker K, Kendziorra K, Becker G, Hesse S, Woelpl D, et al. Reduced alpha4beta2*-nicotinic acetylcholine receptor binding and its relationship to mild cognitive and depressive symptoms in Parkinson disease. Arch Gen Psychiatry 2009;66:866–77.
23. Brody AL, Mandelkern MA, London ED, Olmstead RE, Farahi J, Scheibal D, et al. Cigarette smoking saturates brain alpha(4)beta (2) nicotinic acetylcholine receptors. Arch Gen Psychiatry 2006;63:907–15.
24. Terrière E, Sharman M, Donaghey C, Herrmann L, Lonie J, Strachan M, et al. alpha4 beta2-nicotinic receptor binding with 5-IA in Alzheimer's disease: methods of scan analysis. Neurochem Res 2008;33:643–51.
25. Tzourio-Mazoyer N, Landeau B, Papathanassiou D, Crivello F, Etard O, Delcroix N, et al. Automated anatomical labeling of activations in SPM using a macroscopic anatomical parcellation of the MNI MRI single-subject brain. Neuroimage 2002;15:273–89.
26. Arendt T, Bigl V. Alzheimer's disease as a presumptive threshold phenomenon. Neurobiol Aging 1987;8:552–54.
27. Perry E, Martin-Ruiz C, Lee M, Griffiths M, Johnson M, Piggott M, et al. Nicotinic receptor subtypes in human brain ageing, Alzheimer and Lewy body diseases. Eur J Pharmacol 2000;393:215–22.
28. Nordberg A, Alafuzoff I, Winblad B. Nicotinic and muscarinic subtypes in the human brain: changes with aging and dementia. J Neurosci Res 1992;31:103–11.
29. Pimlott SL, Piggott M, Owens J, Greally E, Court JA, Jaros E, et al. Nicotinic acetylcholine receptor distribution in Alzheimer's disease, dementia with Lewy bodies, Parkinson's disease, and vascular dementia: in vitro binding study using 5-[(125)I]-A-85380. Neuropsychopharmacology 2004;29:108–16.
30. Rinne JO, Myllykylä T, Lönnberg P, Marjamäki P. A postmortem study of brain nicotinic receptors in Parkinson's and Alzheimer's disease. Brain Res 1991;547:167–70.
31. Nordberg A, Lundqvist H, Hartvig P, Lilja A, Långström B. Kinetic analysis of regional (S)(-)11C-nicotine binding in normal and Alzheimer brains—in vivo assessment using positron emission tomography. Alzheimer Dis Assoc Disord 1995;9:21–7.
32. O'Brien JT, Colloby SJ, Pakrasi S, Perry EK, Pimlott SL, Wyper DJ, et al. alpha4beta2 nicotinic receptor status in Alzheimer's disease using 123I-5IA-85380 single-photon-emission computed tomography. J Neurol Neurosurg Psychiatry 2007;78:356–62.
33. Nordberg A, Hartvig P, Lilja A, Vitanen M, Amberla K, Lundqvist H, et al. Decreased uptake and binding of 11C-nicotine in brain of Alzheimer patients as visualized by positron emission tomography. J Neural Transm Park Dis Dement Sect 1990;2:215–24.
34. Ellis JR, Villemagne VL, Nathan PJ, Mulligan RS, Gong SJ, Chan JG, et al. Relationship between nicotinic receptors and cognitive function in early Alzheimer's disease: a 2-[18F]fluoro-A-85380 PET study. Neurobiol Learn Mem 2008;90:404–12.
35. Mitsis EM, Reech KM, Bois F, Tamagnan GD, Macavoy MG, Seibyl JP, et al. 123I-5-IA-85380 SPECT imaging of nicotinic receptors in Alzheimer disease and mild cognitive impairment. J Nucl Med 2009;50:1455–63.
36. Yakushev I, Hammers A, Fellgiebel A, Schmidtmann I, Scheurich A, Buchholz HG, et al. SPM-based count normalization provides excellent discrimination of mild Alzheimer's disease and amnestic mild cognitive impairment from healthy aging. Neuroimage 2009;44:43–50.
37. Giovacchini G, Conant S, Herscovitch P, Theodore WH. Using cerebral white matter for estimation of nondisplaceable binding of 5-HT1A receptors in temporal lobe epilepsy. J Nucl Med 2009;50:1794–800.
38. Terrière E, Dempsey MF, Herrmann LL, Tierney KM, Lonie JA, O'Carroll RE, et al. 5-(123)I-A-85380 binding to the α4β2-nicotinic receptor in mild cognitive impairment. Neurobiol Aging 2010;31:1885–93. doi:10.1016/J.neurobiolaging.2008.10.008.
39. Soonawala D, Amin T, Ebmeier KP, Steele JD, Dougall NJ, Best J, et al. Statistical parametric mapping of (99m)Tc-HMPAO-SPECT images for the diagnosis of Alzheimer's disease: normalizing to cerebellar tracer uptake. Neuroimage 2002;17:1193–202.
40. Staley JK, van Dyck CH, Weinzimmer D, Brenner E, Baldwin RM, Tamagnan GD, et al. 123I-5-IA-85380 SPECT measurement of nicotinic acetylcholine receptors in human brain by the constant infusion paradigm: feasibility and reproducibility. J Nucl Med 2005;46:1466–72.